Planetary Nebulae: An Eye to the Future
Proceedings IAU Symposium No. 283, 2011
A. Manchado, L. Stanghellini & D. Schönberner, eds.

doi:10.1017/S1743921312010976

(F)UV spectral analysis of 15 extremely hot, hydrogen-rich central stars of planetary nebulae

Marc Ziegler[1], Thomas Rauch[1], Klaus Werner[1] and Jeffrey W. Kruk[2]

[1]Institute for Astronomy and Astrophysics, Kepler Center for Astro and Particle Physics, Eberhard Karls University, Tübingen, Germany
email: ziegler@astro.uni-tuebingen.de

[2]NASA Goddard Space Flight Center, Greenbelt, U.S.A.

Abstract. We present results of a (F)UV spectral analysis of 15 hot, hydrogen-rich central stars of planetary nebulae (CSPNe) of DAO-type (A 7, A 31, A 35, A 39, NGC 3587, NGC 6720, NGC 6853, NGC 7293, PuWe 1, Sh 2-174) and O(H)-type (A 36, Lo 1, LSS 1362, NGC 1360, NGC 4361). The sample covers a wide range of parameters ($T_{\rm eff} \approx$ 70–130 kK, $\log g$ = 5.4–7.4). It represents different stages of post-AGB evolution. The derived stellar parameters are crucial constraints for AGB nucleosynthesis and stellar evolutionary calculations. Detailed spectral analyses using fully line-blanketed NLTE model atmospheres including 23 elements from hydrogen to nickel are performed. Additional modeling of the ISM line absorption enables to unambigiously identify nearly all observed lines and to improve both, the photospheric as well as the ISM model.

Keywords. Stars: abundances, stars: AGB and post-AGB, stars: atmospheres, stars: evolution, stars: individual (WD 0500–156, WD 0851+090, WD 1250–226, A 36, WD 1625+280, Lo 1, LSS 1362, CPD–26 389, NGC 3587, NGC 4361, WD 1851+329, WD 1957+225, WD 2226-210, WD 0615+556, WD 2342+806), planetary nebulae: individual (A66 7, A66 31, A66 35, A66 36, A66 39, Lo 1, LSS 1362, NGC 1360, NGC 3587, NGC 4361, NGC 6720, NGC 6853, NGC 7293, PuWe 1, Sh 2-174)

1. Introduction

CSPNe are hot post-AGB stars ionizing the surrounding matter that they previously expelled on the AGB. Hot post-AGB stars represent an important link between the AGB and the WD cooling track, the former being important for the nucleosynthesis. In the last decade, emphasize was laid on the analysis of H-poor post-AGB stars (cf. Werner & Herwig 2006) although the majority ($\approx$ 75 %) of all post-AGB stars is H-rich. Only a few systematic analyses are available in the literature concerning metal abundances of H-rich CSPNe. Good *et al.* (2005) determined abundances for a sample of 16 DAO-type CSPNe from *FUSE* spectra, and Bauer & Husfeld (1995) analyzed a sample of seven sdO stars and four CSPNe.

Metals play a significant role in the analysis of stellar spectra and in stellar evolution. They provide a tool to derive $T_{\rm eff}$ accurately, using the ionization equilibria of successive ionization stages. Metals have many (in the case of iron-group elements millions) of line transitions resulting in a significant impact on the temperature stratification of the stellar atmosphere and, thus, on the determination of other elemental abundances. Metal abundances put constraints on AGB nucleosynthesis calculations. We use high-S/N, high-resolution FUV and UV observations obtained with *FUSE*† and *HST*‡, respectively, to derive basic stellar parameters ($T_{\rm eff}$, $\log g$, chemical composition, mass, luminosity, distance) as well as interstellar properties like $n_{\rm H\,I}$ and $E_{\rm B-V}$.

† Far Ultraviolet Spectroscopic Explorer
‡ Hubble Space Telescope

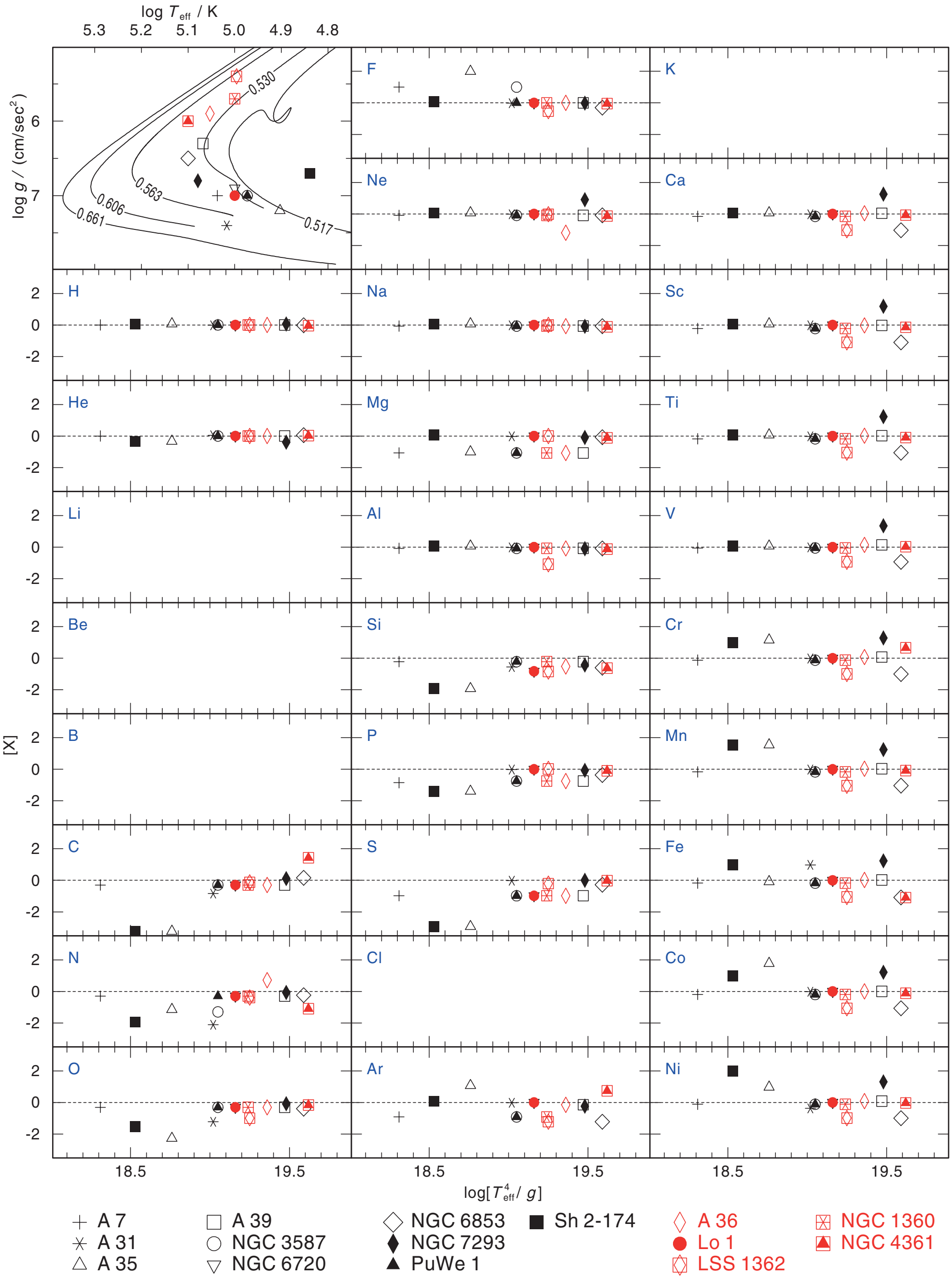

Figure 1. $\log T_{\rm eff} - \log g$ diagram (upper left) and chemical abundances as a function of $\log\,[T_{\rm eff}^4/g]$. DAO-type CS are displayed in black, O(H) types in red. The evolutionary tracks from Miller Bertolami (priv. comm.) are labeled with the stellar masses (in $M_\odot$). [X] denotes log(abundance/solar abundance) for species X.

2. Atmosphere modeling and analysis methods

For the calculation of the photospheric spectrum we employed the Tübingen NLTE Model Atmosphere Package (*TMAP*, Werner *et al.* 2003; Rauch & Deetjen 2003).In

https://doi.org/10.1017/S1743921312010976 Published online by Cambridge University Press

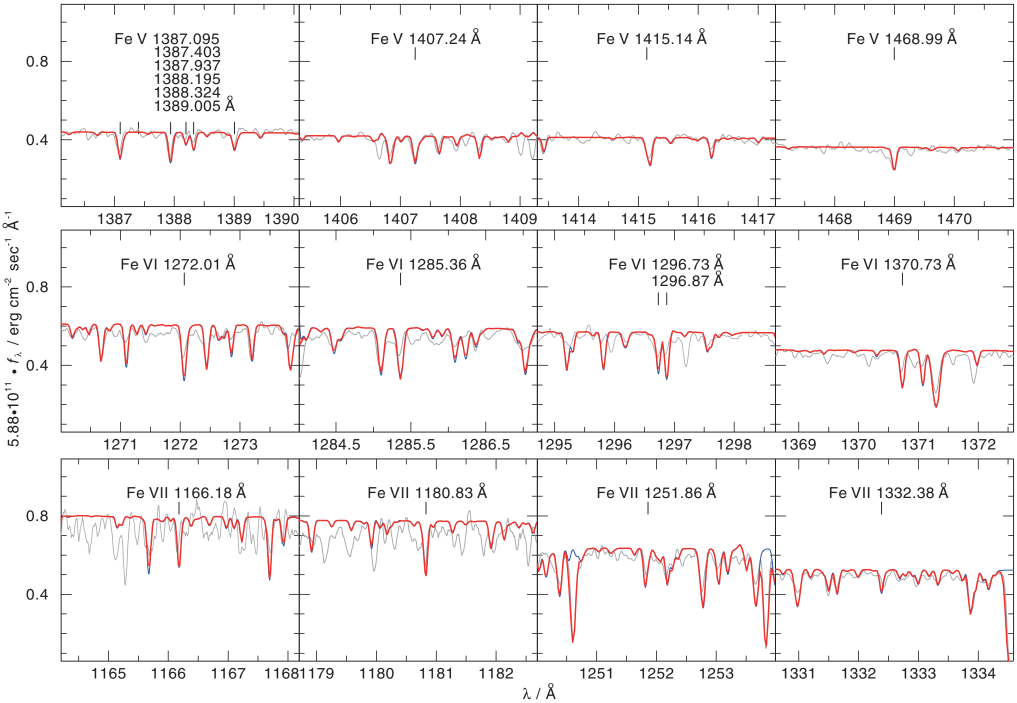

Figure 2. Sections of the *STIS* observation of the CSPN of A 35. The ionization equilibrium of Fe V – VII is used to precisely determine $T_{\rm eff}$ ($T_{\rm eff} = 80$ kK, $\log g = 7.2$).

order to calculate the atmospheric structure reliably, the opacities of 23 elements from H to Ni were considered.

The *FUSE* wavelength range (915 – 1180 Å) is highly contaminated by interstellar absorption features. These hamper the analysis of the photospheric spectrum. We employed *OWENS* to model the interstellar line absorption. As a new standard modeling technique the photospheric and the ISM model SEDs are combined. This allows to improve both, the photospheric and the ISM model. The final photospheric model SEDs will be available via the GAVO† service TheoSSA‡.

For the determination of $n_{\rm H\,I}$ either Ly α (1216 Å, *HST/STIS*) or Ly β (1026 Å, *FUSE*) were analyzed. $E_{\rm B-V}$ was determined using spectra obtained with *FUSE*, *STIS*, *IUE*, as well as photometric data from the optical and infrared. $T_{\rm eff}$ was derived using ionization equilibria, e.g. N IV – V, O IV – VI, Si IV – V, Fe V – VIII (Fig. 2). $\log g$ was determined from fitting the line wings of H I, He II, C IV, and O VI lines. Abundances were measured by detailed line-profile comparison. If lines were strongly blended by the ISM lines, upper limits were determined only.

Stellar masses were determined by comparison of the stars' positions in the $\log T_{\rm eff}$ – $\log g$ diagram with evolutionary tracks of Miller Bertolami (priv. comm.). Distances were then calculated following the flux calibration of Heber *et al.* (1984).

3. Results

Our main results are shown in Tab. 1. As the radiation pressure ($\propto T_{\rm eff}^4$) counteracts the gravitational settling Fig. 1 shows the abundances as a function of $\log(T_{\rm eff}^4/g)$. DAO

† German Astrophysical Virtual Observatory
‡ Theoretical Stellar Spectra Access, `http://dc.g-vo.org/theossa`

https://doi.org/10.1017/S1743921312010976 Published online by Cambridge University Press

Table 1. Main results for the DAO-type (upper part) and O(H)-type CSPNe. The typical error for the mass determination is $\pm 0.05\,\mathrm{M}_\odot$, for $E_{\mathrm{B-V}}$ ± 0.02. The values for m_{V} were taken from the SIMBAD database. For A 35 and Lo 1 m_{V} was derived using model SEDs.

PN	T_{eff} [kK]	$\log g$ [cm/sec^2]	d [pc]	M [$\mathrm{M}_\odot$]	$E_{\mathrm{B-V}}$	m_{V}	$n_{\mathrm{H\,I}}$ [10^{20} cm^{-2}]	v_{rad} [km/sec]
A 7	109	7.0	734^{+226}_{-312}	0.544	0.08	15.45	4.0 ± 1.5	41 ± 17
A 31	94	7.4	421^{+130}_{-180}	0.588	0.09	15.51	1.5 ± 1.5	80 ± 10
A 35	80	7.2	214^{+66}_{-92}	0.521	0.09	13.80	5.0 ± 1.5	-10 ± 10
A 39	117	6.3	1748^{+529}_{-735}	0.533	0.13	15.60	5.0 ± 2.0	30 ± 12
NGC 3587	94	7.0	975^{+299}_{-412}	0.527	0.00	16.04	0.3 ± 0.4	30 ± 12
NGC 6720	100	6.9	440^{+134}_{-186}	0.534	0.08	14.20	3.0 ± 2.0	-19 ± 10
NGC 6853	126	6.5	663^{+201}_{-279}	0.547	0.07	13.70	1.6 ± 0.3	-25 ± 10
NGC 7293	120	6.8	469^{+142}_{-197}	0.538	0.00	13.52	1.3 ± 0.2	-10 ± 10
PuWe 1	94	7.0	365^{+67}_{-37}	0.527	0.21	15.53	2.7 ± 1.4	35 ± 15
Sh 2-174	69	6.7	634^{+260}_{-362}	0.402	0.00	14.74	3.0 ± 0.2	40 ± 10
A 36	108	5.9	451^{+137}_{-190}	0.543	0.07	11.57	6.0 ± 0.5	40 ± 10
Lo 1	100	7.0	754^{+230}_{-322}	0.538	0.00	15.39	0.6 ± 1.4	80 ± 15
LSS 1362	99	5.4	1057^{+322}_{-446}	0.559	0.15	12.50	0.5 ± 0.2	0 ± 10
NGC 1360	100	5.7	499^{+152}_{-210}	0.534	0.00	11.20	0.5 ± 0.1	50 ± 10
NGC 4361	126	6.0	1009^{+305}_{-423}	0.553	0.04	13.20	2.3 ± 0.2	16 ± 10

and O(H)-type CSPNe do not differ in T_{eff} but the O(H)-type stars have lower $\log g$ $(5.4 - 6.0)$ compared to the DAO-type CS $(6.5 - 7.4)$. The exception is Lo 1 ($\log g = 7.0$). The position of the O(H)-type CS in the $\log T_{\mathrm{eff}} - \log g$ diagram shows that they are less evolved than the DAO-type CS. From a comparison of the stellar positions in the $\log T_{\mathrm{eff}} - \log g$ diagram with evolutionary tracks from Miller Bertolami (priv. comm.) a mean mass of $\overline{M} = 0.535\,\mathrm{M}_\odot$ is derived. This is significantly lower than the mean mass for DA and DO-type white dwarfs. However, some objects of our sample are known binary stars. Excluding these (A 7, A 31, A 35, A 39, Sh 2–174) a mean mass of $\overline{M} = 0.540\,\mathrm{M}_\odot$ can be deduced, which is still too low. The derived distances agree well with the literature values.

Acknowledgements

TR is supported by the German Aerospace Center (DLR) under grant 05 OR 0806. This research has made use of the SIMBAD database, operated at CDS, Strasbourg, France. This work used the profile-fitting procedure *OWENS* developed by M. Lemoine and the *FUSE* French Team.

References

Bauer, F. & Husfeld, D. 1995, *A&A*, 300, 481

Good, S. A., Barstow, M. A., Burleigh, M. R., *et al.* 2005, *MNRAS*, 363, 183

Heber, U., Hunger, K., Jonas, G., & Kudritzki, R.-P. 1984, *A&A*, 130, 119

Rauch, T. & Deetjen, J. L. 2003, *ASP-CS*, 288, 103

Werner, K., Deetjen, J. L., Dreizler, S., Nagel, T., & Rauch, T. 2003, *ASP-CS*, 288, 31

Werner, K. & Herwig, F. 2006, *PASP*, 118, 183